

## Investigations of cosmic magnetism at the Crimean Astrophysical Observatory. I. Magnetic field in the interstellar medium and secondary effects of stellar magnetism

R.E. Gershberg, I.Yu. Alekseev, N.I. Bondar'

Crimean Astrophysical Observatory, Nauchny 298409, Crimea  
e-mail: [gershberg@craocrimea.ru](mailto:gershberg@craocrimea.ru)

Submitted on June 5, 2020

### ABSTRACT

We summarize the main results obtained at the Crimean Astrophysical Observatory for the magnetic field of the interstellar medium and magnetism in the middle- and low-mass stars with the solar-type activity.

**Key words:** Galaxy: magnetic fields, stars: middle- and low-mass stars, magnetic activity, starspots, active regions and activity cycles

## 1 Introduction

Cosmic magnetism has been studied at the Crimean Astrophysical Observatory over 75 years since its foundation. The investigations were pioneered at the Simeiz Observatory by its director – academician G.A. Shajn. During several generations Crimean scientists studied magnetism of the interstellar medium, Sun, different-mass stars with the solar-type activity and without it.

Experimental and theoretical studies at CrAO in the middle of the 20th century provided new insights into the interstellar medium structure, the evolution of its individual elements and the general dynamics of the interstellar matter; these encouraged the formation of a new branch of astrophysics in our country – cosmic electrodynamics. Basic publications on this branch were included into the compiled at CrAO collection of works G.A. Shajn. *Selected works* (2012) and S.B. Pikel'ner. *Selected works* (2016).

In 1958, the IAU Committee on Variable Stars singled out red dwarf stars, on which there were recorded high-amplitude sporadic flares and a strong emission spectrum in quiescence, into a separate group of the UV Ceti stars. The unexpected activity of these coolest, known then, dwarf stars caused the necessity of theoretical interpretation, and many theoretical models appeared, up to the “new physics”. But in 1965, the first time-resolved spectra of stellar flares were taken at CrAO; from these spectra the substantial similarities between flares on these red dwarfs and on the Sun were identified (Gershberg, Chugainov, 1966, 1967). Taking into account these findings, as well as the first recorded radio bursts of such stars and stellar-astronomical notions, Gershberg, Pikel'ner (1972) put forward a hypothesis for the physical identity of activity of the flaring red dwarfs and the

solar activity. To date, this hypothesis is a widely accepted basis for the solar-stellar physics and allows one to talk about the solar-type activity of middle- and low-mass stars. In particular, about their magnetism.

The current review reports the basic results derived at CrAO in studying magnetic fields in the Galaxy and secondary effects of magnetism of active stars – starspots, optical emission polarization, emissive active regions and stellar activity cycles.

## 2 Magnetism of the interstellar medium

In the late 40s of the past century, the Observatory on Mount Koshka received from Germany two high-speed F/1.4 Slevogt–Richter cameras – at first the camera with a diameter of 450 mm, and two years later – the 640 mm camera. These instruments, used during the War by the Germans to guard the La Manche coast, were redesigned into astronomical telescopes; for several years G.A. Shajn, V.F. Gase, and their colleagues took photographs in the  $H_{\alpha}$  rays of a region of the Milky Way visible in Simeiz. They developed in detail a procedure for such observations, combining the spectral sensitivity of photographic plates and light filters, then this was widely used abroad. As a result, more than 150 new emission diffuse nebulae were discovered (Gase, Shajn, 1955).

Having analyzed all the known at that time such formations and taking into account their significant diversity, G.A. Shajn and V.F. Gase refused the notion about structureless amorphous nebulae and distinguished among them an important morphological type: massive nebulae with predominant matter in the periphery – in both our Galaxy and

extragalactic systems (Shajn, Gase, 1953). The existence of such structures, first, rejected the hypothesis of the formation of emission nebulae by the matter ejection from stars, since their masses exceeded by a few orders of magnitude the masses of the exciting hot stars, and second, it served as a starting moment for putting forward and elaborating by G.A. Shajn a concept for dynamics of diffuse nebulae and their groups – expanding and disintegration of these formations. Whereas, G.A. Shajn complemented gas-dynamic effects by the influence of the magnetic field of the Galaxy and the magnetic field in diffuse nebulae, as well as by the examples of elongated, predominantly parallel to the galactic equator bright and dark nebulae, by the general orientation of fine filament systems (Shajn, 1955a, b, 1956). When he later confirmed this concept, taking into account properties of the interstellar light polarization of stars, and estimated the direction – at an angle of  $18^\circ$  to the Galaxy plane, and the magnetic field strength of the interstellar medium in close vicinity of the Sun to be about  $10^{-5}$  oersted (Shajn, 1955b, 1957), the initial hypothesis of the existence of the interstellar medium magnetic field proved to be a convincing fact. A detailed analysis of distribution of the interstellar light polarization planes allowed him to ascertain the positions of galactic arms.

Having entered in 1946 at the Simeiz Observatory, S.B. Pikel'ner proceeded with theoretical studies on solar physics and took part in spectroheliographic observations. He was immediately inspired with respect to observations, observing the way G.A. Shajn through comparatively simple facilities derived interesting and far-reaching conclusions associated with the structure and evolution of gaseous nebulae. And G.A. Shajn involved him into these works. Among a number of studies carried out with G.A. Shajn or under his influence, four papers of Pikel'ner were related to magnetism of the interstellar medium.

First, following Alfvén's opinion that the cosmic ray isotropy may be due to by the magnetic field of the Galaxy, S.B. Pikel'ner (1953) put forward and elaborated a concept of the galactic halo: a uniform gas-dynamic spherical structure of the low-density ionized magnetized gas, in which near the equator the higher-density discrete clouds float due to the magnetic field that is in dynamic equilibrium with the gas; the sonic speed in the halo exceeds the speed of clouds, their motions remain subsonic and thus maintain their identity for a long time. S.B. Pikel'ner derived a self-consistent picture of the galactic halo at a speed of the intercloud gas of 50 km/s, a density of its particles of  $0.1 \text{ cm}^{-3}$ , and a magnetic field strength of more than  $3 \cdot 10^{-6}$  oersted. This concept attracted a significant interest, and soon halos were detected by radioastronomers in extragalactic systems.

Second, in cooperation with G.A. Shajn, S.B. Pikel'ner elaborated a hypothesis of turbulent motions of matter in the Orion Nebula based on brightness fluctuations. In the framework of this hypothesis they assessed the magnetic field strength in it to be  $3 \cdot 10^{-4}$  oersted (Pikel'ner, Shajn, 1953).

Third, after identifying by I.S. Shklovsky optical emission of the Crab Nebula with the synchrotron radiation of energetic electrons in the magnetic field, this object attracted much attention, and S.B. Pikel'ner (1956) considered in detail the process of arising this scintillation based on the hypothesis of the continuous production of relativistic particles from the star. He showed the emission of electrons in the

magnetic field to lead to an increase by unit, starting from some energy, a spectral index in the distribution of their emission, and position of this spectrum fracture is determined by the magnetic field strength. Making use of this circumstance, S.B. Pikel'ner estimated the magnetic field strength in the center of the Crab Nebula to be  $5 \cdot 10^{-4}$  oersted and  $3 \cdot 10^{-4}$  oersted on average for a nebula. The proposed by S.B. Pikel'ner model of energetic particles diffusion in the magnetic field made it possible to interpret acceleration of the nebula shell and variations of its color from the center to the periphery. Later, such a method of magnetic field estimation has been widely used when studying other radio sources.

Forth, following Shajn's conclusion about galactic arms as about structures associated with the magnetic field, S.B. Pikel'ner and L.P. Metik (1958) compared a character of line-of-sight velocities of interstellar clouds within  $\pm 20^\circ$  from the galactic equator towards directions that are perpendicular to the Cassiopeia–Perseus arm, parallel to the same arm in Cygnus and parallel to the arm in Sagittarius and found that the fast motion components of clouds show a higher speed dispersion along arms than across; this confirms the effect of the field on the gas motion.

Simultaneously with researches, S.B. Pikel'ner was actively involved in the arising then new science – cosmic electrodynamics. In the book *Theoretical astrophysics* edited by V.A. Ambartsumyan he wrote a large section “Electrodynamics of the solar atmosphere” (Pikel'ner, 1952), then the review “Electromagnetic phenomena in astrophysics” (Pikel'ner, 1954). In Simeiz S.B. Pikel'ner began to write one of the first course books *Fundamentals of cosmic electrodynamics*, which was later published as a second edition in Russian, was translated into English and published by NASA.

### 3 Magnetism of stars with the solar-type activity

#### 3.1 Starspots

Dark spots on the Sun are structures with high-strength local magnetic fields. Thus, the investigation of starspots is a way of studying stellar magnetism. In CrAO the first starspots were revealed by P.F. Chugainov (Chugainov, 1966) from observations of the binary system of red dwarfs BY Dra; later he detected spottedness in stars with the solar mass and in objects with various evolution status – from young stars that recently left the T Tauri stage up to the strongly evolved giants of the asymptotic branch (Chugainov, 1976). The *UBVRI* observations of over three dozens of spotted stars of different types are currently being carried out at CrAO (Kozhevnikova, Alekseev, 2015; Alekseev, Kozhevnikova, 2017, 2018).

During the first decades, numerous patterns from the analysis of photometry of the spotted stars resulted in estimates of coordinates, sizes, and temperature of one-two and in some cases – of three spots. These reported nothing about stellar magnetism and gave a picture quite dissimilar to the solar spottedness with its numerous sunspots.

So far, a spectral method of the Doppler mapping has gained a wide distribution in studying stellar spottedness. There exist several algorithms of this method, but all of them may be applied to only bright stars with noticeable rotation so

that with a definite reliability to estimate intensity of the comparably narrow spectral line region, which is well widened by the rotation. This constraint is substantial for the weak flaring stars.

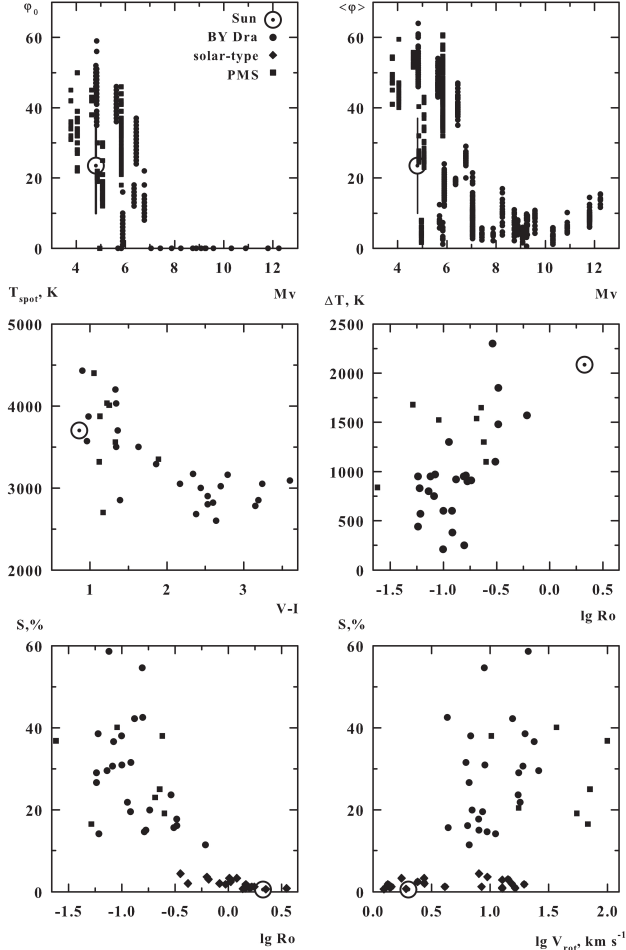


**Fig. 1.** Comparison of the calculated parameters of the zonal spottedness models of active dwarf stars – the distance of the spottedness band from the equator  $\phi_0$ , the middle latitude of spots  $\langle\phi\rangle = \phi_0 + \Delta\phi/2$ , the spot temperature  $T_{spot}$ , the difference between the temperature of the photosphere and spots  $\Delta T$ , the degree of spottedness of the stellar surface  $S$  – with the global stellar parameters: the absolute stellar magnitude  $M_V$ , the rotation rate  $v_{rot}$  and the Rossby numbers. The figure takes into account data on the models of 25 BY Dra stars (994 epochs), 8 young stars that left the T Tauri stage (171 epochs), and 21 low-active solar-type stars (Alekseev, 2014; Alekseev, Kozhevnikova, 2017, 2018; Bruevich, Alekseev, 2007)

Contrary to the mentioned photometric and spectral methods for the analysis of the spotted photosphere, in which there was posed a challenge of ascertaining parameters of individual spots, Alekseev, Gershberg (1996, 1997) suggested performing a search for the general properties of stellar spotted regions, a so-called zonal spottedness model. In the simplest zonal spottedness model, a photometric effect of a set of starspots is approximated – following the pattern of sunspots – by two symmetric regarding the equator dark

bands with a variable width in longitude, and such a model is described by four free parameters: the distance of dark bands from the equator, their two extreme widths and a ratio of the surface starspot brightness and the unperturbed stellar photosphere. Note that algorithms for modeling of a spot have also four free parameters.

Within the framework of such a zonal spottedness model, Alekseev (2001) uniformly analyzed observations of 25 red dwarf stars for over 340 observational epochs. This analysis was applied to stars in the spectral type range from dG1e to dM4.5e with rotation rates between several units and 25 km/s. The sought-for parameters of the zonal models turned out to be in the following range: distances of the spottedness bands from the equator are from 0 to 55°, widths of these bands – from 0.5° to 34°, and the temperature parameter  $\beta_V$  – from 0.03 to 0.58. Consequently, the considered models described stellar spottedness in an interval between 2 and 50 % of their total surface (Alekseev, 2001).

The zonal spottedness model included four free parameters and described only symmetric light curves, whereas practically all the spotted stars, involving the Sun, exhibits the presence of two active longitudes. Trying to remove this shortcoming, Alekseev (2008) examined the zonal spottedness model with a more complicated, two-humped character of the band widths in longitude: he introduced two additional parameters for the dependence of the band occupation density by spots on the longitude – physically this means the consideration of two active longitudes on the star – and yielded extreme points of light curves for 25 stars in 679 epochs with an accuracy of at least 0.<sup>m</sup>01. However, the recomputed four parameters of models have not practically changed; this follows from the ratios between homonymous parameters averaged on all the stellar epochs: the regression coefficients between these values differ from unit by 0.003–0.035. Thus, the account of the second active longitude, resulting in some improvement of the insight into the observed light curves, has not practically changed values of the model parameters.

The number of the considered observational epochs was further on increased and a list of the explored objects was enlarged by young stars that left the T Tauri stage (Alekseev, 2014; Alekseev, Kozhevnikova, 2017, 2018). Aside from dwarf stars, the zonal model has been successfully applied to the modeling of the spotted RS CVn and FK Com giants (Kozhevnikova, Alekseev, 2015).

Results of the zonal modeling of dwarf stars are outlined in Fig. 1, which yields the comparison of the derived parameters of zonal models with global stellar characteristics: their absolute magnitudes  $M_V$ , rotation rates  $v_{rot}$  and Rossby numbers  $Ro$  that are equal to a ratio of the axial rotation period of the star to the characteristic time of convective vortex circulation; the encircled dot denotes the middle position of the Sun in these plots, and vertical segments in two top plots mark ranges of the corresponding solar values. This figure exhibits not plots from the monography of (Alekseev, 2001), but results of their further development in subsequent years (Alekseev, 2014; Alekseev, Kozhevnikova, 2017, 2018; Bruevich, Alekseev, 2007).

Dependencies presented in Fig. 1 made it possible to draw conclusions which could not be inferred from the mapping of individual spots by traditional methods. These dependencies provide information on some general magnetic field properties of these stars.

A comparison of the middle latitude of spots and the absolute luminosity showed that the spotted regions on all the stars are localized at low and middle latitudes, whereas there is a clear tendency for the presence of spots towards the equator in cooler stars: the average width of spots does not exceed  $20^\circ$  in late K and M dwarfs. For hotter stars, spots are shifted towards middle latitudes and occupy a larger latitudinal interval. In other words, for stars with the absolute luminosity  $M_V > 7^m$ , calculations reveal the merging of two spottedness bands assumed symmetric with respect to the equator into one structure. For a half of the hotter stars, calculations yielded two bands, as on the Sun. Stars with split spottedness bands demonstrate a tendency to a growth of  $\phi_0$  towards brighter stars, including the Sun. The BE Cet star, the most similar to the Sun, reveals the minimum width of the spottedness band  $\Delta\phi$ ; this corresponds to the situation that is the most similar to the solar one.

The temperature of the spotted regions varies from 4000 K for solar-type stars and 2500–3000 K for the coolest M dwarfs. The correlation coefficient of values on the corresponding plot is  $r(T_{spot}, M_V) = 0.69 \pm 0.08$ . A comparison of the temperature differences of the photosphere and the spot  $\Delta T$  with global stellar parameters showed that, on average, this difference achieved 2000 K for hot and 300 K for cool stars. In addition, one can suggest a statistical growth of  $\Delta T$  with a growth of the Rossby number: the correlation coefficient is  $r(\Delta T, \lg Ro) = 0.67 \pm 0.05$ .

The maximum areas of the spotted regions tend to grow with increasing stellar rotation rate and with a decrease of the Rossby number. However, taking into account the dependence  $Ro(v_{rot})$ , the two latter plots in Fig. 1 cannot be considered independent ones.

According to the statistics of 113 spotted red dwarf stars, [Alekseev \(2000\)](#) found that the photometric variability weakly depends on the spectral type and amplitude of the rotational modulation, and amplitudes of seasonal fluctuations of the mean brightness increase with a growth of the stellar rotation rate and with a decrease of the Rossby numbers, achieving the saturation near a velocity critical value of 15–20 km/s and a Rossby number of about 0.2–0.3. The Sun falls well into the detected dependencies (Fig. 1).

Thus, in all the plots of Fig. 1 the solar spottedness parameters falls into the regions occupied by parameters of the zonal spottedness models or into the natural extension of these regions. Otherwise, there is a clear tendency to join the parameters of the calculated zonal models with the solar spottedness characteristics. This fact suggests that the derived stellar zonal spottedness models actually reflect the essential properties of the surface inhomogeneity of red dwarfs.

The Crimean concept of zonal spottedness led to interesting results on the general problems of physics of flaring stars. The extracted estimates for values of stellar spottedness and spot temperature made it possible to assess the bolometric deficit of radiation of the spotted photosphere ([Alekseev et al., 2001](#)). When comparing a value of the bolometric deficit with the total chromospheric radiation and radiation of corona in X-rays, a definite correlation was detected (Figs. 2 and 3); in Fig. 2 the correlation coefficient is  $r = 0.86 \pm 0.07$ , in Fig. 3  $r = 0.78 \pm 0.17$ . Thus, there is a magnetic connection of subphotospheric regions, where the spots form, with upper layers of stellar atmospheres. For the most active dKe stars, the bolometric deficit of photospheric

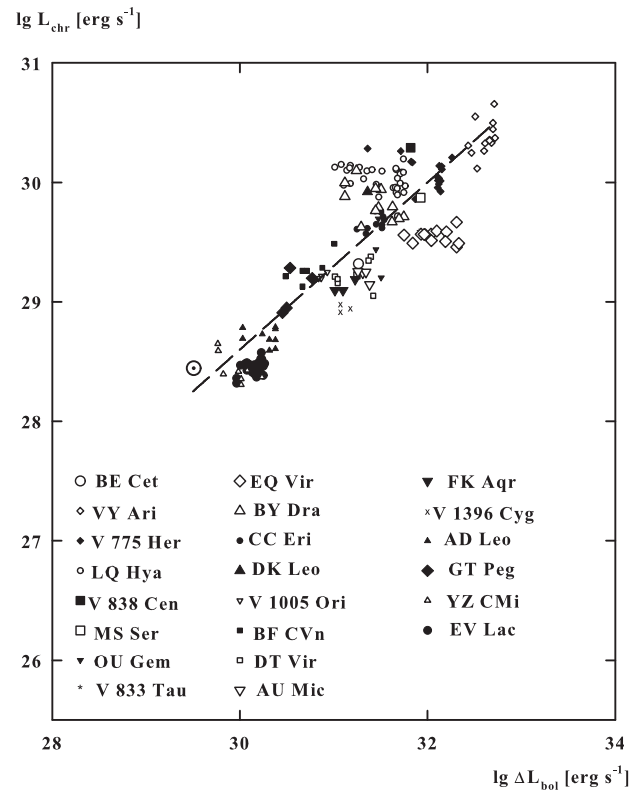


**Fig. 2.** Comparison of the X-ray radiation of stellar coronae and bolometric deficit of the stellar photosphere radiation ([Alekseev et al., 2001](#))

radiation achieves 30 % of the bolometric luminosity and in absolute units it is from  $3 \cdot 10^{29}$  to  $5 \cdot 10^{32}$  erg/s. Obviously, this substantial variable flow needs to be taken into account when considering energetics of the stellar atmosphere.

Thereafter, of particular interest is a qualitatively new result obtained in 2003 by the Moscow colleagues Livshits and Katsova coauthored with Alekseev ([Livshits et al., 2003](#); [Katsova et al., 2003](#)): for several most heavily spotted stars, for which zonal models are calculated, the separate spottedness belts were detected in different hemispheres, and there was found a systematic shift of lower borders of these belts to the equator as the activity cycle developed; i.e., within the concept of Crimean zonal spottedness models for six red dwarfs they plotted diagrams of spot drifts, analogous to solar Maunder butterfly diagrams, and determined the differential rotation of these stars. The rates of the spot zone drift for these stars proved to be 2–3 times lower than those on the Sun.

[Bruevich, Alekseev \(2007\)](#) estimated the spottedness degree for a series of stars with activity close to the solar one and found that the spottedness value exceeds the solar level from 0.3 % to 1–5 % for stars of the HK project and then strikingly increases up to 20–35 %. They revealed a tight correlation between the spot area and power of the stellar X-ray radiation with different activity levels.

Regardless of results of the Doppler mapping, which by the number of works prevails when considering stellar spottedness, the photometric mapping is still relevant. First, the

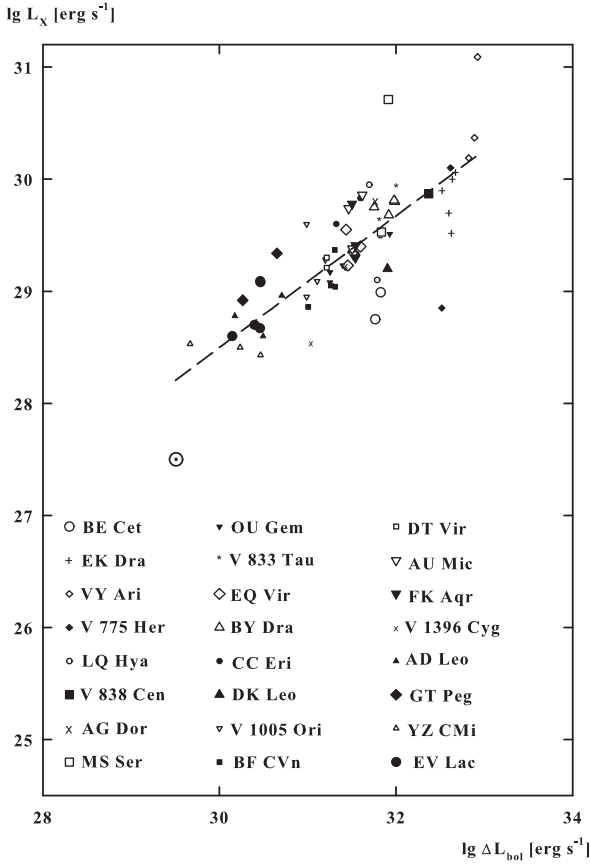


**Fig. 3.** Comparison of the stellar chromosphere emission and bolometric deficit of the stellar photosphere radiation (Alekseev et al., 2001)

photometric investigations span more long-term periods and, consequently, are more appropriate for searching for activity cycles, differential rotation and other long-term effects. Second, a part of stars, having low rotation rates, are actually inaccessible to the Doppler mapping, and just photometric studies are applicable for searches for the statistical dependencies of stellar spot parameters in a wide range of global stellar characteristics. Third, the final result of the Doppler mapping is substantially affected by the selection of lines under investigation, by the accurate determination of the stellar rotation rate and inclination angle of its axis, the selection of atmosphere model parameters, the contribution of chromospheric activity, a successful choice of the integration grid, etc. And finally, fourth, looking at the results of the Doppler mapping of the same input data, but acquired by various methods, one may only be surprised by the repeated statements that the results of the Doppler mapping are weakly dependent on the used method for solving an inverse task: under a close consideration the Doppler mapping is still a sort of art, whereas a more rough estimate of spottedness parameters from photometric observations within the zonal model is free from the required numerous additional input data and ambiguousness in the selection of a calculation method.

However, it is worth noting that the Doppler mapping often leads to the high-latitude and even polar spots; this has not been derived with the zonal model. This provides

evidence for the necessity of further improving the stellar zonal spottedness model.

### 3.2 Broadband linear polarization of red dwarf stars

Similar to sunspots, the spotted regions of red dwarf stars have strong enough, 1–4 kGs, local magnetic fields which trigger the Zeeman splitting and absorption line polarization in the spectrum of a star. When making photometric observations in *UBVRI* broad bands, an effect of the lines within the band is summarized, and consequently the radiation of the star is weakly polarized. Dollfus (1958) and Leroy (1962) discovered this effect of magnetic saturation directly for the emission of sunspots. Thus, a rather simple method is proposed that does not require highly dispersed spectral observations to estimate the local magnetic fields of starspots (Huovelin, Saar, 1991; Saar, Huovelin, 1993).

To the first successful polarimetric observations of active dwarfs there belong the results obtained by Huovelin et al. (1985, 1988, 1989) at the 1.25 m telescope AZT-11 of the Crimean Observatory with the Pirola *UBVRI* photometer-polarimeter, which was designed in cooperation with employees of CrAO N.M. Shakhovskoy and Yu.S. Efimov. In addition to the variable star, a comparison star and some polarization standards were observed every night. One measurement of the star comprised eight exposures in each filter that correspond to eight positions of the plate  $\lambda/2$ . For these eight positions there were compared radiation intensities in two diaphragms, corresponding to perpendicular polarized usual and unusual rays. For each position of the polarizer *I*, in all the filters one may obtain the parameter  $Q_i = n_{eord,i}/n_{ord,i} < Q_i >$ , and then the Stokes parameters  $P_x = (Q_1 + Q_5 - Q_3 - Q_7)/8$ , and  $P_y = (Q_2 + Q_6 - Q_4 - Q_8)/8$ . Such a technique, with the enough number of calculations, allows one to achieve in calculating the Stokes parameters  $P_x$  and  $P_y$  an accuracy of about 0.04% in the *U* band, about 0.03% in the *B* and *V* bands, and 0.02% in the *R* and *I* bands.

For a dozen of solar-type stars, including the well-known spotted star BE Cet, Huovelin et al. (1985, 1988, 1989) revealed a reliable linear polarization of radiation and its rotational modulation, which was compared to variability of emission lines of CaII HK. Since all the program objects are the nearest solar-type stars from the Gliese catalogue, the contribution of interstellar polarization is negligible.

In 1996–2002 this program was continued. Alekseev (2003), Alekseev, Kozlova (2003a), Alekseev, Kozlova (2002, 2003b) carried out *UBVRI* linear-polarization observations of the four known spotted stars MS Ser, VY Ari, LQ Hya, EK Dra, having a later spectral type and a higher activity level than the stars from the sample of Huovelin et al. (1985, 1988, 1989). The observations were performed at AZT-11 with the same equipment and using the same technique.

An application of the  $\chi^2$  test to observational results showed that for all the program stars there were observed real variations of the Stokes parameters from night to night (Alekseev, 2003). A growth of the polarization degree from the *I* to *U* band is clearly seen. The Stokes parameters showed the rotational modulation in the *U* band with the axial rotation period of the star (Fig. 4). The amplitude of the rotational modulation of the Stokes parameters in the approximation of two Fourier harmonics is up to several tenths of a per cent

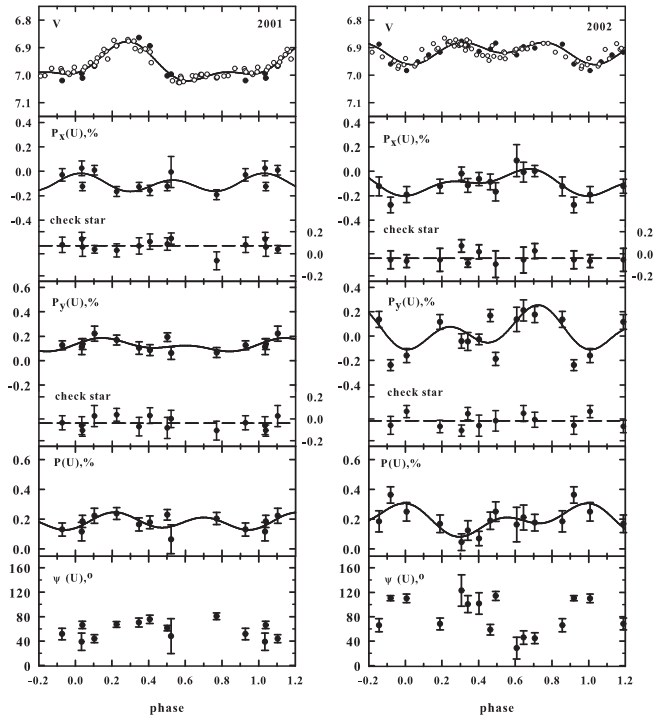


**Fig. 4.** Rotational modulation of brightness in the V band, the Stokes parameters of the active young star VY Ari and those of the check star in the U band, the degree and position angle of the linear polarization of VY Ari in the U band. Dots denote Crimean observations, empty circles – data from the Catania Observatory (Alekseev, 2003)

(MS Ser). For other photometric bands the linear polarization is lower.

Fig. 4 demonstrates an example of developing the degree and polarization angle in the U band folded in phase with the light curve. The figure shows that the polarization degree maximum is shifted with respect to the brightness minimum by some value of  $\Delta\phi$ , comprising 0.05–0.45 of the period and which is characteristic of local magnetic fields located near the most spotted longitudes (Huovelin, Saar, 1991).

The wave dependence of the observed linear polarization degree  $P_s$  is fairly characteristic of the magnetic saturation mechanism – a combination of the Zeeman polarization effect of lines within the certain photometric band. Such an effect is dominating for dwarf stars, whereas the contribution of the Rayleigh and moreover Thompson scattering in the inhomogeneously illuminated atmosphere may be neglected. Following the calculations by Huovelin, Saar (1991) and Saar, Huovelin (1993), the maximum theoretically expected value of the polarization degree in the U band is achieved with a local magnetic field strength of about 1 kGs, typical of sunspots, and with a filling factor of the magnetized active region of about 60%. The observed linear polarization degree is in good agreement with this value (Alekseev, 2003).

Fig. 5 represents the dependence of the observed linear polarization degree in the U band on the color index  $B - V$

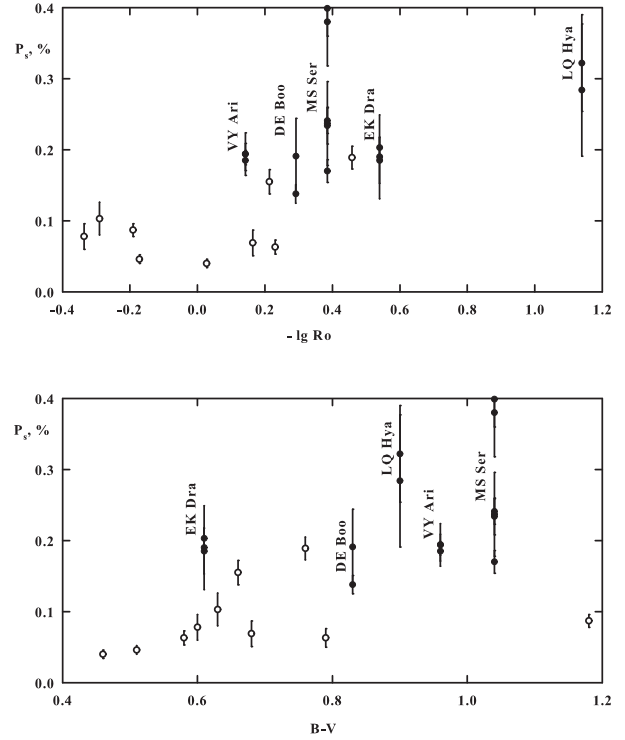


**Fig. 5.** Dependence of the observed linear polarization degree of Alekseev's program stars (dots) and stars from Huovelin et al. (1985, 1988, 1989) (empty circles) on the color index and the Rossby number (Alekseev, 2003)

and the Rossby number for Alekseev's program stars and stars from Huovelin et al. (1985, 1988, 1989). The figure exhibits a growth of the observed polarization towards later spectral types and smaller Rossby numbers, i.e. towards stars with a higher rotation rate and, evidently, with higher magnetic activity. Such dependence seems to be analogous to the detected by Saar (1996) dependence of the magnetic flux of active stars on the same variables.

### 3.3 Emission active regions

Emission lines of hydrogen and ionized calcium doublet – the second characteristics, aside from sporadic flares, the presence of which in 1958 came into the determination of flaring UV Cet-type red dwarf stars. As early as in the middle of the past century, the intensity modulation of the calcium emission lines was detected associated with rotation of stars, having inhomogeneities in the longitudinal distribution of emission regions. It was naturally to identify such regions with stellar chromospheres, therefore the increased magnetic field strengths in active regions of the solar chromosphere and the given above Fig. 2 provide a basis for considering this emission as a secondary effect of stellar magnetism. Based on the emission spectra studies actively carried out at CrAO, the first quantitative characteristics of stellar chromospheres were acquired.

Spectrograms of EV Lac and AD Leo in their quiescent states were derived with the two-camera spectrograph SP-

72 mounted in the Nasmyth focus of ZTSh. The extracted relative intensities of Balmer lines from  $H_\beta$  to  $H_9$  were in good agreement with the Balmer decrement of the solar chromosphere at a height of several tens of kilometers above the solar limb (Fig. 6). Then making use of spectrograms taken with other spectrographs of ZTSh, we estimated absolute energy fluxes in the Balmer lines of five red dwarfs:  $F_{Ba} = (2 \div 4) \cdot 10^6 \text{ erg/cm}^2\text{c}$ ; this exceeds by a factor of 2 the corresponding value of the solar chromosphere (Gershberg, 1970).

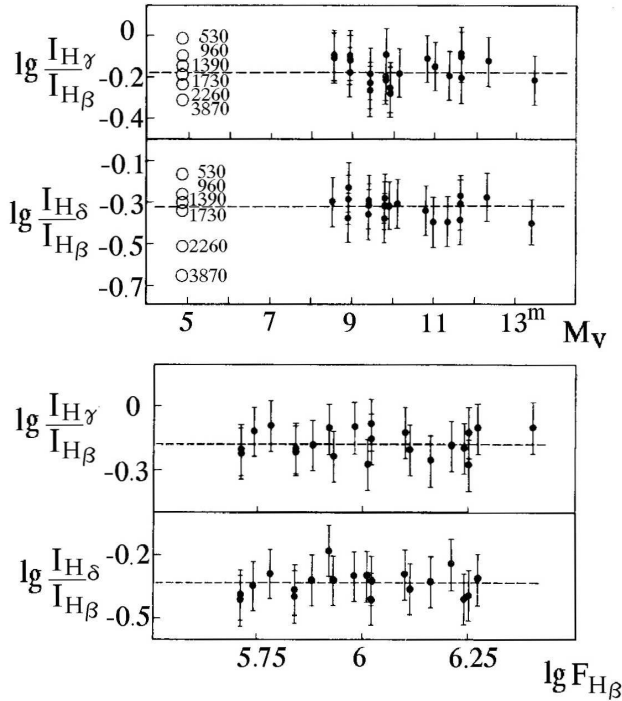


**Fig. 6.** Intensity ratios of the Balmer lines in spectra of the quiet red dwarfs depending on the absolute luminosity  $M_V$  and the absolute luminosity of the  $H_\beta$  line. Circles denote the corresponding values in the spectrum of the solar chromosphere derived at different heights during spectrography at different phases of the solar eclipse (Shakhovskaya, 1974)

Shakhovskaya (1974) derived over hundred spectrograms of 43 active dwarfs in quiescence using SP-72 and first compiled an extensive report on equivalent widths and relative intensities of emission lines for such objects. The emission Balmer decrement in spectra of the quiet red dwarfs was revealed to be invariable in the range of stellar absolute values from  $8.^m5$  to  $13.^m5$  (Fig. 6) and close to the decrement of the middle solar chromosphere. This figure exhibits a practical independence of parameters of stellar chromospheres from characteristics of photospheres. On the other side, N.I. Shakhovskaya detected a positive correlation between the energy radiated by the stationary chromosphere and that radiated by flares. The lower the stellar luminosity, the more contribution in its resulting radiation may be introduced by flares and the stationary chromosphere.

For the interpretation of the observed Balmer emission decrement in spectra of flaring stars at CrAO, within the Sobolev concept of moving stellar envelopes, the Balmer

decrement calculations were carried out for the case of purely collisional excitation of hydrogen lines in an isothermal gas free of external radiative influence. Despite the noticeable distinctions of this model from the stellar chromosphere, these calculations were applied to the Balmer decrements recorded in the quiescent states of nine flaring stars. This resulted in the first estimates of the characteristic electron densities of stellar chromospheres:  $(1 \div 4) \cdot 10^{12} \text{ cm}^{-3}$  at an assumed temperature of 10000 K (Gershberg, 1974). Then Grinin (1979) added photospheric radiation, but this almost did not affect the estimates of electron densities. Satisfactorily presenting the observed decrement, the concept of moving envelopes required noticeable internal movements in the radiating medium with velocities up to 20–30 km/s, which had not been observed. This fact raised doubts about the validity of the extracted density estimates. Later, Katsova (1990) (GAISH) elaborated the theory of Balmer decrement free of the assumption on the substantial motion in the radiating medium: the quantum exit was achieved not by the differential motion of matter, but due to the quantum frequency drift at multiple scattering and their diffusion in the wings of line profiles. An application of this theory to the observed decrements yielded the density estimates that exceeded the above estimates approximately by a factor of 2.

From spectra of the flaring red dwarf EV Lac in the quiet state acquired with ZTSh in 1994 and 1995, the average emission profiles of  $H_\alpha$ ,  $H_\beta$  and  $H_\gamma$  were extracted, and based on these data Baranovsky, Gershberg, and Shakhovskoy (2001) calculated a semiempirical model of the quiet stellar chromosphere. The calculation was performed by selecting such temperature distribution with height, at which the calculated emission line profiles have the best fit to the observed ones, and the variation of density with height is determined by the hydrostatic equilibrium; an additional condition is the absence of the He I  $\lambda$  4471 Å line. To calculate profiles, the Crimean program elaborated by E.A. Baranovsky was used based on the theory of line formation in the absence of LTE. Calculations were performed for three variants: under the assumption of forming emission lines of the chromosphere, being uniform over the stellar surface, and under the assumption that the recorded emission spectrum is radiated by active regions, which occupy one-half and one-third of the stellar surface. Results of the calculations are presented in Fig. 7 where the mentioned variants are marked by numbers 1, 2, and 3. The figure shows the existence in the stellar chromosphere of a wide temperature plateau at a level of 6500–7000 K that resembles the analogous structure in the solar chromosphere. Vertical straight lines delimit regions where 80% of fluxes in the  $H_\alpha$  and  $H_\beta$  lines of the stellar chromosphere are formed, i.e. they are principally formed on the plateau, and the electron density in this region is within the range from  $10^{12}$  to  $3 \cdot 10^{10} \text{ cm}^{-3}$ ; this is approximately by an order of magnitude lower than their previous estimates. Structures of the calculated models of active regions differ from models of the homogeneous chromosphere of the star by a remarkably higher optical thickness in hydrogen lines, by a higher – 500–1500 K – temperature of matter on the plateau, and at more depth by a rise to the high-temperature region. Hydrogen emissions began to form practically at the same depths as in the model of the homogeneous chromosphere, but in models of active regions they extend higher, to smaller values of  $m$ , which correspond to the mass of an in-

dividual column of the above atmosphere. Electron densities in the models of active regions are by a factor of 2–4 higher than those in the model of the homogeneous chromosphere, approaching to the estimate of this value on the Balmer decrement. Thus, these calculations satisfactorily represented the observed profiles and equivalent widths of  $H_\alpha$ ,  $H_\beta$ , and  $H_\gamma$ , and the absence in the spectrum of the helium line  $\lambda 4471 \text{ \AA}$ . For the Sun, the temperature plateau is localized at a height from 1200 to 1800 km, and for EV Lac – from 200 to 700 km, i.e. noticeably deeper, closer to the surface of the star.

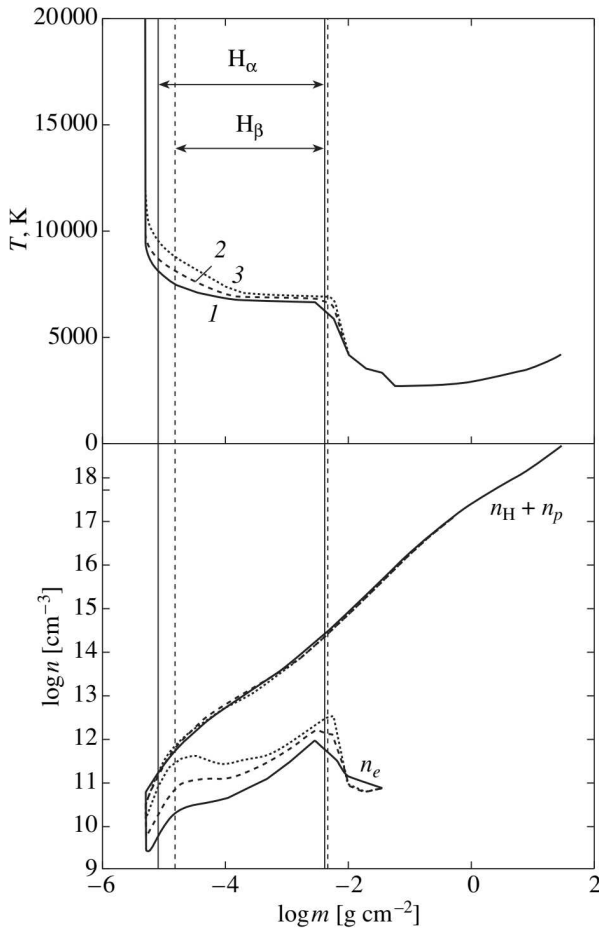


**Fig. 7.** Models of the homogeneous chromosphere for EV Lac (1) and active regions covering one-half (2) and one-third (3) of the stellar surface (Baranovskii et al., 2001)

Since 1998 Alekseev and Kozlova have carried out regular high-resolution spectral observations of four chromospheric active spotted stars V775 Her, LQ Hya, MS Ser, VY Ari at ZTSh (Alekseev, Kozlova, 2000, 2001, 2003a, 2002, 2003b). In the mentioned articles for all these stars there was detected a rotational modulation of equivalent widths of the  $H_\alpha$  line, intensities of its emission double peaks and the distance between them. A comparison with the simultaneously obtained light curves of stars has shown that for all these stars the maxima of the equivalent width and emission intensity correspond to the phases of the minimum brightness, i.e. coincide in longitude with the most spotted regions. Whereas there simultaneously occurs a growth of the elec-

tron density from  $n_e = 1 \cdot 10^{10} \text{ cm}^{-3}$  to  $n_e = 5 \cdot 10^{10} \text{ cm}^{-3}$  for V775 Her, from  $1.1 \cdot 10^{11} \text{ cm}^{-3}$  to  $2.4 \cdot 10^{12} \text{ cm}^{-3}$  for LQ Hya, from  $3.7 \cdot 10^{11} \text{ cm}^{-3}$  to  $3.1 \cdot 10^{13} \text{ cm}^{-3}$  for MS Ser, and from  $1 \cdot 10^{10} \text{ cm}^{-3}$  to  $4.6 \cdot 10^{11} \text{ cm}^{-3}$  for VY Ari. This effect indicates the presence of active regions (focculae) with a high electron density in chromospheres of the investigated stars; these regions concentrate at the same active longitudes as the most spotted regions. Later observations allowed one to suspect the long-term variability of activity in the  $H_\alpha$  line. In particular, for the young star VY Ari, the long-term variations of emission parameters of  $H_\alpha$  show the cyclicity with a characteristic time of 9–10 years, which coincides with a characteristic cycle of spot activity of this star. Moreover, for this variable, there were observed qualitative variations of the  $H_\alpha$  line profile from season to season – from the two-component emission to the slightly embedded by emission absorption profile with the same characteristic time (Alekseev et al., 2020).

### 3.4 Activity cycles in the middle- and low-mass stars

The most long-term secondary effects of stellar magnetism with a characteristic time ranging in years and decades are activity cycles of stars. Suspicions about their existence were reported as early as in the beginning of the past century Hale had discovered strong magnetic fields in sunspots. The first direct experimental data on stellar cycles were obtained by Olin Wilson (Wilson, 1978) as a result of the many-year monitoring of H and K lines of ionized calcium in spectra of 91 stars in the lower part of the main sequence.

Based on the Crimean BY Dra observations in the  $B$  and  $V$  bands, Chugainov (1973) suspected a 8–9-year cycle of the spot-formation activity on this star. Phillips, Hartmann (1978) analyzed brightness of four late dwarfs from photographic achieves of Harvard Observatory and for two of them detected activity cycles with a duration of several decades. Similar investigations at CrAO were made by Bondar' (1995), Bondar (1996, 2001). In the photographic collections of GAISH MSU, Odessa University Observatory and Sonneberg Observatory she studied the behavior of average annual brightness of 40 dKe-dMe stars having magnitudes of 7–15<sup>m</sup>. From results of measurements by the eye and with the iris photometer of about 5900 negatives obtained between 1896 and 1992, the long-term variations in annual brightness with amplitudes from 0.<sup>m</sup>3 to 1.<sup>m</sup>0 and a characteristic time from 3 to 60 years were found for 21 stars. Amplitudes of more than 0.<sup>m</sup>5 were detected for four red dwarfs: V 833 Tau, PZ Mon, EI Cnc and BY Dra. Later, PZ Mon was ascertained to belong to RS CVn-type variables (Pakhomov et al., 2015). A significant number of objects studied by Bondar' allowed us to make the preliminary statistical conclusions on the cyclic activity of stars. Fig. 8 represents the comparison of the estimated by Bondar' parameters of cyclicity with other stellar characteristics. Following Fig. 8a, activity cycles with large duration are produced in stars with rotational periods of less than 5 days. Figs. 8b and 8c show that amplitudes of average annual brightness of more than 0.<sup>m</sup>5 are observed on stars with a duration of cycles of over 30 years and with a luminosity in soft X-rays of higher than  $3 \cdot 10^{29} \text{ erg/s}$ , whereas these high values of  $L_X$  are mainly found for K dwarfs of the sample.



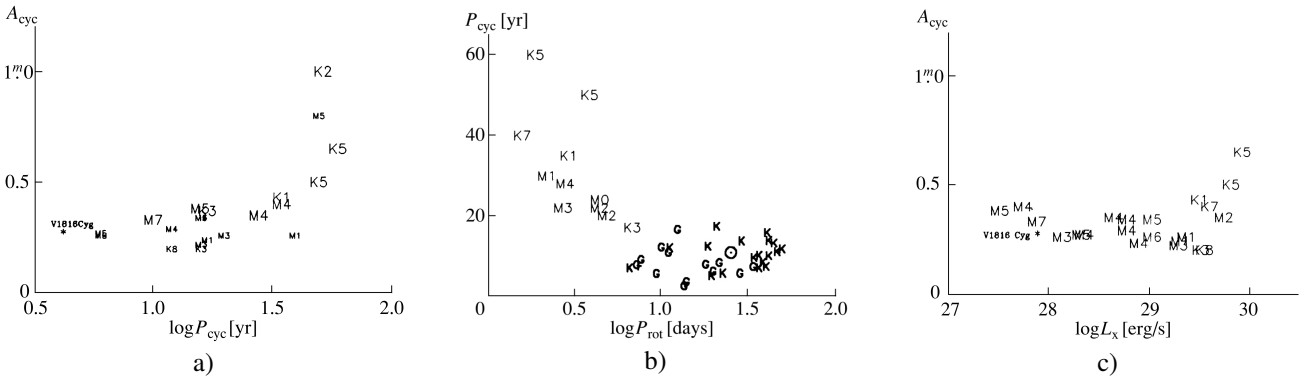


**Fig. 8.** Comparison of characteristics of the long-term brightness variations and global properties of the red dwarf stars: (a) duration of activity cycles and amplitudes of optical brightness; (b) rotational periods and duration of activity cycles; (c) luminosities of K and M dwarfs in soft X-rays and amplitudes of optical brightness ([Bondar', 2002](#))

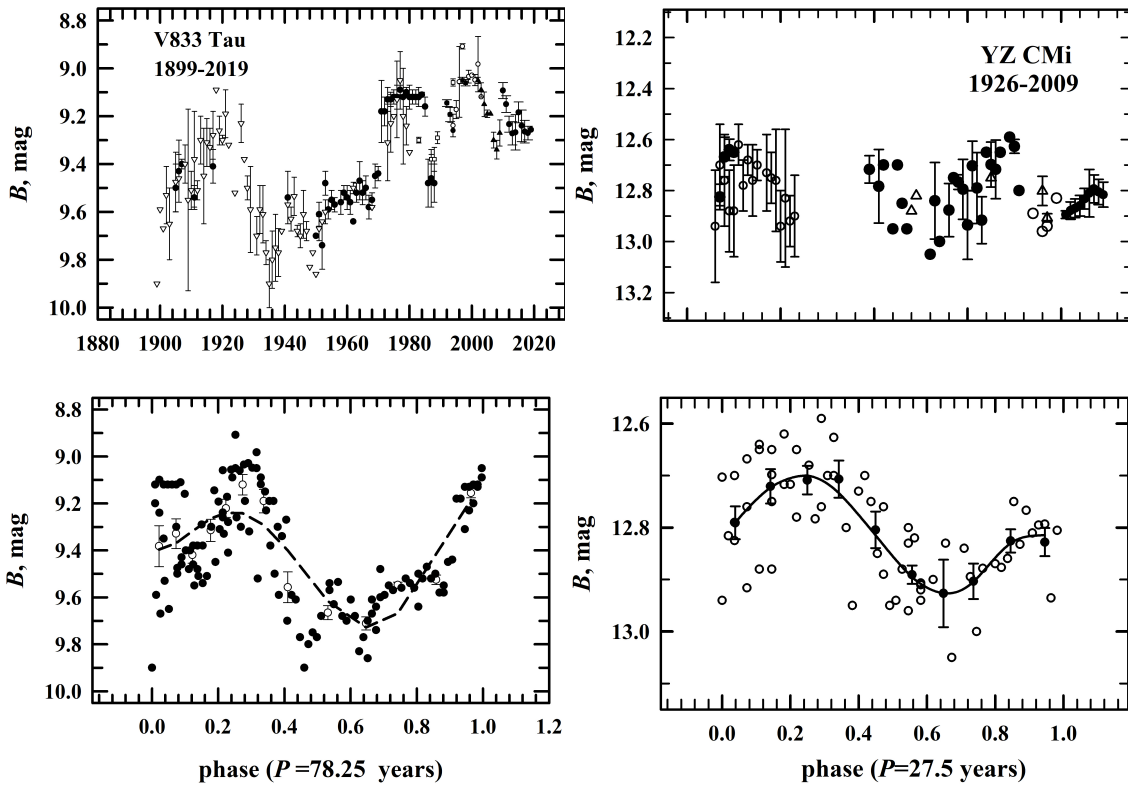


**Fig. 9.** Long-term variations in brightness of active red dwarfs and cyclic character of their variability

By further consideration of her sample of stars, [Bondar \(2013\)](#) took into account the coexistence of short and long cycles of activity in many of them and suggested that they are generated by different dynamos, operating in different layers of the star.

In 1992–2004, a program of photometric observations in *UBVRI* bands was carried out at the 1.25 m telescope AZT-11 of CrAO using the five-channel photometer-polarimeter with a goal to find or confirm a cyclical activity on some stars: V833 Tau, DT Vir, V1396 Cyg, PZ Mon, YZ CMi, etc. ([Alekseev, Bondar', 1997, 1998; Alekseev, 2001; Alekseev, Bondar', 2006; Bondar', 2015; Bondar, Katsova, 2018](#)). A study of the photospheric activity of stars is cur-

rently carried out on the analysis of long-term light curves which combined measurements in photographic archives, photometric data obtained at automated telescopes and with wide-field cameras ([Alekseev, Kozhevnikova, 2017; Bondar, 2019](#)). Fig. 9 exhibits the most complete light curves and main activity cycles for two active red dwarfs – V833 Tau ([Bondar', 2015; Bondar' et al., 2019](#)) and YZ CMi ([Bondar, Katsova, 2018](#)).

To study parameters of the cycles and their relationship with the physical characteristics of stars, [Bondar \(2019\)](#) has formed a sample of 65 G–M dwarfs, whose cycles were determined from the series of observations of activity indices for 30 years or more. Such a sample, including 14 G dwarfs,

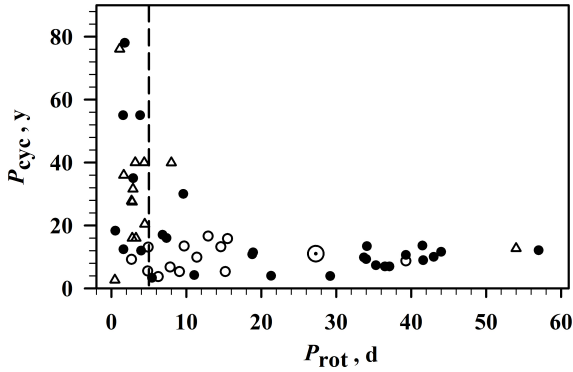


**Fig. 10.** Durations of activity cycles of G–M dwarfs and a different character of the relation between ( $P_{cyc}$ ) and ( $P_{rot}$ ) for stars with rotation periods more and less than 5 days

28 K dwarfs, and 23 M dwarfs, allows one to jointly consider the main cycles for solar-type stars and active red dwarfs, involving also rapidly rotating late M stars. Activity cycles with duration from 2 to 80 years were revealed for 61 stars. For almost a half of stars (48%), cycles are comparable with the Schwabe solar cycle, for 15 objects cycles are short, less than 7 years, for V833 Tau and V647 the longest cycles are suspected – about 80 years (Bondar, 2019; Bondar’ et al., 2019, 2020).

Besides the main cycle, some G–M dwarfs show in variations of chromospheric and photospheric indices of activity one or several short cycles with a smaller amplitude, the nature of which has no straightforward interpretation. The duration of secondary cycles is from 2 to 10 years, but there are stars with cycles of more than 10 years, for instance, for V833 Tau – a 19-year cycle (Bondar’, 2015), and for AU Mic – 13–16 years (Bondar’ et al., 2020).

For stars with long periods, there is a tendency for increasing the cycle length with a declining of the rotation rate. However, in this group there are distinguished dwarfs with rotation periods of 7–20 days, which have more steep dependence of the cycle length on the rotation rate than for stars, rotating slower than the Sun (Katsova et al., 2015). These are young and more active stars.

From a sample of 65 stars with rotation periods from fraction of a day to 60 days, it has been convincingly shown that the threshold value, distinguishing G–M dwarfs into two groups, is a rotation period of 5 days – see Fig. 10 that refines Fig. 8a (Bondar’ et al., 2020). According to this figure, for stars with  $P_{rot} > 5$  days the cycle length increases with a decreasing of the rotation rate, whereas for old stars, rotating slowly than the Sun, this tendency is expressed weaker than for young G- and K dwarfs with  $5 < P_{rot} < 20$  days, and cycles more than 20–22 years have not been revealed for them. Among young K dwarfs there are known stars with cycles up to 40 years. The Sun is located between sequences of old and young stars.

On the rapidly rotating stars, the longest cycles are observed, but no definite association with the rotation period is traced. The cycle amplitude for the solar-type stars does not exceed  $0.2^m$ , and for the fast rotating cool dwarfs it increases up to  $0.5^m$  and higher; this points to a high level of spottedness of their photospheres in the activity maximum. K

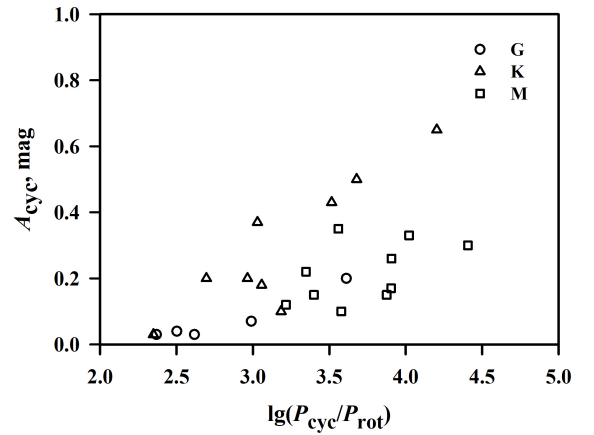


**Fig. 11.** Relationship between the amplitude and duration of the cycle for G–M dwarfs with different rotational periods

dwarfs are distinguished among G and M dwarfs by duration and amplitude of their cycles (Fig. 11).

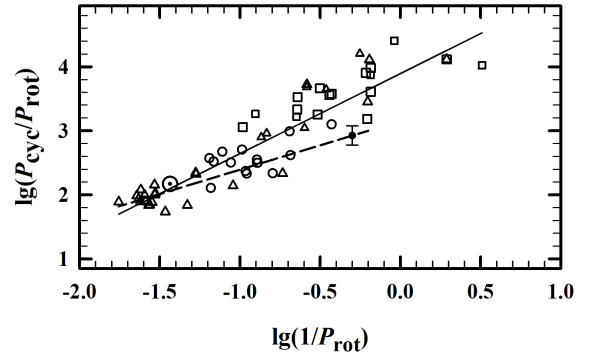


**Fig. 12.** Dependence between the cycle length and the rotation period for G–M dwarfs. Symbols are the same as in Fig. 10, the solar symbol denotes the location of the Sun in the plot (Bondar’ et al., 2020)

Baliunas et al. (1996) have shown that the relation between the theoretical number of dynamo  $D$  and the number of rotations in a cycle  $P_{cyc}/P_{rot}$  is expressed by the power law  $P_{cyc}/P_{rot} \sim D^i$ . The logarithmic diagram suggested by them is used for determining parameter  $i$  for various samples of stars and conditions for action of the unified dynamo mechanism. For the solar-type stars, following Vida et al. (2014),  $i = 0.76 \pm 0.15$  (the dashed line in Fig. 12), based on the array of 65 stars  $i = 1.25 \pm 0.068$  (Bondar, 2019; Bondar’ et al., 2020). A significant difference of the value  $i$  compared to the previous investigations may be explained by a large fraction of rapidly rotating dwarfs in this sample. An investigation of the cycles of activity of stars using the results obtained from the described above models of zonal spottedness was carried out in Alekseev (2004), Alekseev (2005, 2014) and Alekseev, Kozhevnikova (2017, 2018). Out of more than three dozens of the considered stars, for 17 of them, including 12 red dwarfs, a cyclicity of middle latitudes and total areas of starspots was revealed; the detected cycles have durations from 4 to 30 years, whereas the

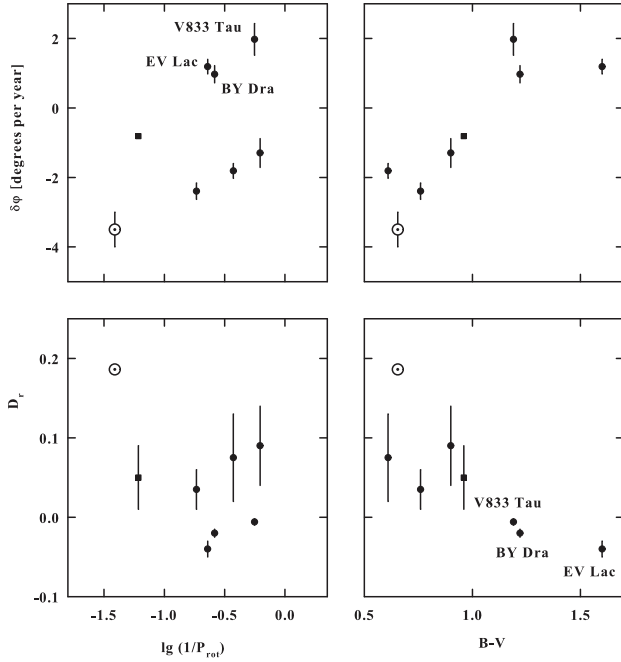


**Fig. 13.** Dependence of the latitude drift speed of the spottedness bands  $\delta\phi$  and the differential rotation coefficient  $D_r$  on the angular velocity of the stellar rotation  $1/P_{rot}$  and the color index  $B - V$  (Alekseev, 2005)

durations of cycles found based on middle latitudes and on areas of spots are in good agreement with each other and with photometric observations. For four dwarf stars (V833 Tau, BY Dra, V775 Her, PZ Mon), such relatively short cycles coexist with cycles of 60–80 years – possible analogs of Gleisberg’s secular solar cycle. The areas of spots in the depth of such cycles sometimes exceed a half of the total stellar surface. Durations of cycles show no distinct dependence on the spectral type of a star, on the rotation rate and the Rossby number.

For 9 stars a rough analogue of the solar butterfly diagram was detected – a decrease of the middle latitude with increasing areas, whereas for the coolest 19 dwarfs, a reverse picture is observed – a growth of spot latitudes with increasing areas, i.e. a drift of spots to the pole as they develop. For 13 stars, a rate of the latitude drift of spots  $\delta\phi$  was assessed. It varies from cycle to cycle and from star to star: from  $-0.8$  to  $-2.6$  degrees per year for a drift of spots towards the equator and from  $0.2$  to  $1.6$  degrees per year for a drift towards the pole, whereas on the Sun this value is from  $-3$  to  $-4$   $^{\circ}/\text{yr}$  (Alekseev, Kozlova, 2019; Alekseev et al., 2019).

For a series of objects, simultaneously with a latitude drift of spots during the cycle, there are smooth variations in the photometric period of the stellar rotation or long-term variations of the position of active longitudes (primary and secondary photometric minima). Such an effect is associated with the differential rotation of a star, which may be both solar-type (the equatorial zone rotates faster than the circum-polar one, the differential rotation coefficient  $D_r = \Delta\Omega/\Omega_{eq}$  is positive) and antisolar-type (the coefficient  $D_r$  is negative). In works of Alekseev (2004), Alekseev (2005) and Alekseev, Kozhevnikova (2017, 2018) on the basis of the

zonal model, the differential rotation estimates were extracted for more than a dozen of stars of various types.

A comparison of the derived from models middle latitudes of spots with photometric periods of the star (or phases of its minimum brightness) has shown the presence of the differential rotation of both types for the program stars. Differential rotation coefficients are on average  $D_r = 0.01$ – $0.05$  for the young post T Tau stars of the spectral type K,  $0.03$ – $0.09$  for G–K dwarfs,  $-0.01$ – $-0.04$  for the spotted M dwarfs, whereas the solar value  $D_{r\odot} = 0.19$ . The character of the differential rotation and that of the latitude drift of spots seem to depend on the spectral type of the star, and transition to the antisolar rotation pattern occurs when achieving some critical value of the color index  $B - V$  (Fig. 13).

For some objects, in particular for the “young Sun” LQ Hya, an effect of switching active longitudes (flip-flop effect), which happens both cyclicly for the LQ Hya, AB Dor stars and irregularly for the VY Ari star. Durations of switching cycles of active longitudes do not coincide with the spottedness cycle, but correspond as whole numbers  $P_{cyc}/P_{flip-flop} = 3 : 1, 2 : 1, 3 : 2, 5 : 4$ , etc. In particular, for the Sun  $P_{\odot cyc}/P_{flip-flop} = 3 : 1$ .

Baklanova, Plachinda (2015) explored the Sun and 27 F9–K7 dwarfs with the known rotation periods and stable one-component activity cycles and estimated the mean speed of the meridional flows that is equal to  $5.4 \pm 1.5$  m/s; this within the error limits corresponds to the mean value for the Sun 6.29 m/s. For this sample there was found the absence of dependence between the detected mean speed of the meridional flow and the Rossby number, which is a parameter-indicator of dynamo mechanisms. Thus, the conclusion was made that the basic mechanism determining the duration of activity cycles is a speed of meridional flows.

## 4 Conclusion

In the middle of the past century, academician G.A. Shajn with colleagues put forward and elaborated a technique for the large detection of diffuse emission nebulae. 150 such objects were discovered, and in the course of their morphological and dynamical analysis there was ascertained an influence of the interstellar magnetic field on these structures. In particular, the strength estimates of such fields were obtained, as well as their ratios with spiral arms of the Galaxy, orientation of the field in the close vicinity of the Sun. Simultaneously with these pioneer experimental works, S.B. Pikel’ner developed quantitative methods for studying the interstellar medium, put forward a concept of the galactic halo and wrote the first in the country works on cosmic electrodynamics.

Throughout decades the Crimean astrophysics of the succeeding generations began extensive investigations of secondary effects of the magnetic field for middle- and low-mass stars with the solar-type activity.

Researchers from CrAO offered and elaborated an original stellar zonal spottedness model which, contrary to the foreign photometric and spectral models oriented on a search for the parameters of individual starspots, was aimed at determining characteristics of the total stellar spottedness. In the framework of this model, about three dozen active stars in a wide range of spectral types were analyzed; the characteristic latitudes, temperatures, and areas of their spotted

regions were assessed; systematic shifts of these regions to the low latitudes were revealed for cooler stars; a decrease of differences in temperatures of spots and the unperturbed photosphere for such stars was detected; a correlation of the spot temperature and the absolute magnitude was suspected; a convincing correspondence of photospheric characteristics of the solar active photosphere with characteristics of stellar spottedness was first detected. Within the zonal spottedness model, the bolometric deficits of emission of stellar spotted photospheres were first estimated, and a convincing correlation of these values with the chromospheric and coronal emission was detected. This observational fact suggests that there is an extension of magnetic lines of force from the sub-photospheric regions to the most upper atmospheric layers of active stars. The zonal spottedness model of active stars made it possible for a series of objects to construct analogues of the Maunder butterflies and to estimate the differential rotation.

The broadband linear polarimetry of a series of active stars revealed a significant polarization up to one-tenth fractions of a percent, which may be attributed to the resulting Zeeman effect of the spectral line splitting in a magnetic field of about 1 kGs. Our foreign colleagues took part in these investigations at the Crimean telescope AZT-11. In active regions of the Sun associated with local magnetic fields, the emission of lines of ionized calcium and hydrogen is observed. Therefore, emissions of these lines in spectra of active stars should be considered as secondary effects of stellar magnetism. Spectral observations at CrAO of dozens of active stars yielded the first quantitative results on stellar chromospheres. Based on these observational data, the first estimates of stellar chromosphere densities were derived; the practical independence of the Balmer decrement from the photosphere radiation in the range of  $M_V$  from  $8^m$  to  $13^m$  and from the absolute luminosity of the emission spectrum was found; the proximity of the stellar Balmer decrement to the decrement of the solar middle chromosphere was detected. To make direct estimates of characteristic densities of chromospheres of active stars, the calculations of radiation within the Sobolev theory of moving envelopes were performed at CrAO. Later calculations refined the gained in Crimea results less than by an order of magnitude.

Based on the spectra of one of the most active flare stars EV Lac, models of its quiet chromosphere were constructed for various coverage of the stellar surface by active regions, as well as models of the active chromosphere with flares. Whereas a significant correspondence of the considered and observed emission line profiles of hydrogen and ionized calcium was achieved. Many-year photometric and spectral observations of several active stars revealed a definite correlation of appearing on them starspots and active regions.

Investigations of stellar activity cycles based on photometric series with duration of about a century were carried out at CrAO. These covered four dozen stars, thus the conclusions on the statistical properties of stellar activity cyclicity were first drawn: the characteristic durations of cycles were estimated, as well as the dependence of cycles' duration on the stellar rotation period and the cycle amplitude on its duration; a relation between the cycle amplitude and the X-ray emission intensity of the stellar corona was determined. These studies carried out on the border of centuries were later repeatedly refined, but the basic conclusions were retained:

long-term activity cycles up to 80 years are characteristic of stars with rotation periods up to 5 days, the highest brightness amplitudes in cycles are typical of stars with cycles of dozens of years and with significant radiation in X-rays. In a sample of 65 stars, the cycles with duration from 2 to 80 years were detected for 61 stars; for a series of the explored stars, besides the cycles with duration of 7–18 years, which can be regarded as analogues of the solar 11-year cycle, the shorter cycles down to 2 years were revealed. This circumstance may be caused by the coexistence of various dynamo mechanisms of magnetic field generation. The brightness amplitude in a cycle of the solar-type stars does not exceed  $0.2^m$ , whereas for the rapidly rotating stars it reaches  $0.5^m$ .

Among more than three dozen stars, for which zonal spottedness models were constructed, for 17 of them activity cycles of middle latitudes of spots and those of their total areas were detected. Contrary to the Sun, for the coolest stars, there was revealed a drift of spots during a cycle from the equator to the pole.

Based on 27 F9–K7 dwarfs, there was estimated the average speed of meridional flows that seem to be associated with a drift of the dipole field during the activity cycle. This value turned out to be 5.4 m/s, whereas on the Sun – 6.29 m/s.

Investigations of the secondary effects of magnetism for the middle- and low-mass stars with the solar-type activity are continued up to date.

The current review was partially reported on October 5, 2016 at the international conference “Physics of stars: from collapse to collapse” held at the Special Astrophysical Observatory RAS and was published in [Gershberg \(2017\)](#).

**Acknowledgements.** The idea to compile the current review belongs to S.I. Plachinda. The authors acknowledge him for the initiative and discussion of findings. Thanks are given to the anonymous referee for useful comments, to Z.A. Taloverova for the help in technical preparation, and to Ya.V. Poklad for preparing the English version of the paper.

## References

- Alekseev I.Yu., 2000. *Astron. Rep.*, vol. 44, no. 10, p. 696.
- Alekseev I.Yu., 2001. *Low-Mass Spotted Stars*. Odessa: As-troprint.
- Alekseev I.Yu., 2003. *Astron. Rep.*, vol. 47, p. 430.
- Alekseev I.Yu., 2004. *Solar Phys.*, vol. 224, p. 187.
- Alekseev I.Yu., 2005. *Astrophysics*, vol. 48, p. 20.
- Alekseev I.Yu., 2008. *Izv. Krymsk. Astrofiz. Observ.*, vol. 104, p. 272.
- Alekseev I.Yu., 2014. *Astrophysics*, vol. 57, p. 254.
- Alekseev I.Yu., Bondar' N.I., 1997. *Astron. Lett.*, vol. 23, p. 257.
- Alekseev I.Yu., Bondar' N.I., 1998. *Astron. Rep.*, vol. 42, p. 655.
- Alekseev I.Yu., Bondar' N.I., 2006. *Astron. Astrophys. Trans.*, vol. 25, iss. 2–3, p. 247.
- Alekseev I.Yu., Gershberg R.E., 1996. *Astron. zhurn.*, vol. 73, p. 589.
- Alekseev I.Yu., Gershberg R.E., 1997. *Astron. Rep.*, vol. 41, p. 207.
- Alekseev I.Yu., Gershberg R.E., Katsova M.M., Livshits M.A., 2001. *Astron. Rep.*, vol. 45, p. 482.

- Alekseev I.Yu., Kozhevnikova A.V., 2017. *Astron. Rep.*, vol. 61, p. 221.
- Alekseev I.Yu., Kozhevnikova A.V., 2018. *Astron. Rep.*, vol. 62, p. 396.
- Alekseev I.Yu., Kozlova O.V., 2000. *Astrophysics*, vol. 43, p. 245.
- Alekseev I.Yu., Kozlova O.V., 2000. *Astrophysics*, vol. 44, p. 429.
- Alekseev I.Yu., Kozlova O.V., 2002. *Astron. Astrophys.*, vol. 396, p. 203.
- Alekseev I.Yu., Kozlova O.V., 2003a. *Astrophysics*, vol. 46, p. 28.
- Alekseev I.Yu., Kozlova O.V., 2003b. *Astron. Astrophys.*, vol. 403, p. 205.
- Alekseev I.Yu., Kozlova O.V., 2019. XVI Young Scientists' Conference, Irkutsk, p. 3.
- Alekseev I.Yu., Kozhevnikova A.V., Kozlova O.V., 2019. Proceedings of the 48th International Conference, Ekaterinburg: UrFU, p. 7.
- Alekseev I.Yu., Kozlova O.V., Gorda S. Yu., 2020. *Astrophys. Bull.*, in press.
- Baklanova D., Plachinda S., 2015. *Adv. Space Res.*, vol. 55, p. 817.
- Baliunas S., Nesne-Ribes E., Sokoloff D., Soon W.H., 1996. *Astrophys. J.*, vol. 460, p. 848.
- Baranovskii E.A., Gershberg R.E., Shakhovskoi D.N., 2001. *Astron. Rep.*, vol. 45, pp. 67–74.
- Bondar' N.I., 1995. *Astron. Astrophys. Suppl. Ser.*, vol. 111, p. 259.
- Bondar N.I., 1996. *Bull. Crim. Astrophys. Observ.*, vol. 93, p. 95.
- Bondar N.I., 2001. *Bull. Crim. Astrophys. Observ.*, vol. 97, p. 13.
- Bondar' N.I., 2002. *Astron. Rep.*, vol. 46, p. 489.
- Bondar N.I., 2013. *Izv. Krymsk. Astrophys. Observ.*, vol. 109, p. 123.
- Bondar' N.I., 2015. *Astron. Rep.*, vol. 59, p. 221.
- Bondar N.I., Katsova M.M., 2018. *Geomagn. Aeron.*, vol. 58, p. 910.
- Bondar N.I., 2019. *Astron. Astrophys. Trans.*, vol. 97, p. 13, in press.
- Bondar' N.I., Gorbunov M.A., Shlyapnikov A.A., 2019. *ASP Conf.*, vol. 518, p. 180.
- Bondar' N.I., Katsova M.M., Livshits M.A., 2020. *Geomagn. Aeron.*, vol. 59, p. 832.
- Bruevich E.A., Alekseev I.Yu., 2007. *Astrophysics*, vol. 50, p. 187.
- Chugainov P.F., 1966. *Inf. Bull. Var. Stars*, no. 122, p. 1.
- Chugainov P.F., 1973. *Izv. Krymsk. Astrofiz. Observ.*, vol. 48, p. 3.
- Chugainov P.F., 1976. *Izv. Krymsk. Astrofiz. Observ.*, vol. 54, p. 89.
- Dollfus A., 1958. *Comptes Rendus*, vol. 246, p. 3590.
- Huovelin Ju., Linnaluoto S., Piirola V., et al., 1985. *Astron. Astrophys.*, vol. 152, p. 357.
- Huovelin Ju., Saar S.H., Tuominen I., 1988. *Astrophys. J.*, vol. 329, p. 882.
- Huovelin Ju., Linnaluoto S., Tuominen I., Virtanen H., 1989. *Astron. Astrophys. Suppl.*, vol. 78, p. 129.
- Huovelin Ju., Saar S.H., 1991. *Astrophys. J.*, vol. 374, p. 319.
- Gase V.F., Shajn G.A., 1955. *Izv. Krymsk. Astrofiz. Observ.*, vol. 15, p. 11.
- Gershberg R.E., 1970. *Astrofizika*, vol. 6, p. 191.
- Gershberg R.E., 1974. *Sov. Astron.*, vol. 18, p. 326.
- Gershberg R.E., 2017. *Izv. Krymsk. Astrofiz. Observ.*, vol. 113, no. 1, pp. 36–77.
- Gershberg R.E., Chugainov P.F., 1966. *Astron. zhurn.*, vol. 43, p. 1168.
- Gershberg R.E., Chugainov P.F., 1967. *Astron. zhurn.*, vol. 44, p. 260.
- Gershberg R.E., Pikel'ner S.B., 1972. *Comments Astrophys. Space Phys.*, vol. 4, p. 113.
- Grinin V.P., 1979. *Izv. Krymsk. Astrofiz. Observ.*, vol. 59, p. 154.
- Katsova M.M., 1990. *Sov. Astron.*, vol. 34, p. 614.
- Katsova M.M., Bondar N.I., Livshits M.A., 2015. *Astron. Rep.*, vol. 59, p. 726.
- Katsova M.M., Livshits M.A., Belvedere G., 2003. *Solar Phys.*, vol. 216, p. 353.
- Kozhevnikova A.V., Alekseev I.Yu., 2015. *Astron. Rep.*, vol. 59, p. 937.
- Livshits M.A., Alekseev I.Yu., Katsova M.M., 2003. *Astron. Rep.*, vol. 47, p. 562.
- Leroy J.L., 1962. *Ann. Astrophys.*, vol. 25, p. 127.
- Pakhomov Yu.V., Chugai N.N., Bondar' N.I. et al., 2015. *Mon. Not. Roy. Astron. Soc.*, vol. 446, iss. 1, p. 56.
- Phillips M.J., Hartmann L., 1978. *Astrophys. J.*, vol. 224, p. 182.
- Pikel'ner S.B., 1952. In Ambarzumian V.A. (Ed.), *Theoretical Astrophysics*. Moscow: GITTL, p. 284.
- Pikel'ner S.B., 1953. *Doklady Akad. nauk*, vol. 88, p. 229.
- Pikel'ner S.B., 1954. *Uspekhi astron. nauk*, vol. 6, p. 281.
- Pikel'ner S.B., 1956. *Astron. zhurn.*, vol. 33, p. 785.
- Pikel'ner S.B., 1961. *Fundamentals of Cosmical Electrodynamics*. Moscow: Fizmatlit.
- Pikel'ner S.B., 2016. *Selected Works*. Moscow: Fizmatlit.
- Pikel'ner S.B., Metik L.P., 1958. *Izv. Krymsk. Astrofiz. Observ.*, vol. 18, p. 198.
- Pikel'ner S.B., Shajn G.A., 1953. *Doklady Acad. nauk*, vol. 90, p. 741.
- Saar S.H., 1996. In Uchida Y. et al. (Eds), *IAU Colloquium 153. Magnetodynamic Phenomena in the Solar Atmosphere*, Dordrecht: Kluwer, pp. 367–374.
- Saar S.H., Huovelin Ju., 1993. *Astrophys. J.*, vol. 404, p. 739.
- Shajn G.A., 1955a. *Astron. zhurn.*, vol. 32, p. 381.
- Shajn G.A., 1955b. *Doklady Acad. nauk*, vol. 101, p. 437.
- Shajn G.A., 1956. *Astron. zhurn.*, vol. 33, p. 305.
- Shajn G.A., 1957. *Astron. zhurn.*, vol. 34, p. 3.
- Shajn G.A., Gase V.F., 1953. *Astron. zhurn.*, vol. 30, p. 135.
- Shajn G.A., 2012. *Selected Works*. Kyiv: Naukova dumka, p. 629.
- Shakhovskaya N.I., 1974. *Izv. Krymsk. Astrofiz. Observ.*, vol. 51, p. 92.
- Vida K., Oláh K., Szabo R., 2014. *Mon. Not. Roy. Astron. Soc.*, vol. 441, p. 2744.
- Wilson O.C., 1978. *Astrophys. J.*, vol. 226, p. 379.